

https://dspace.org/

Analysing spatial data via geostatistical methods

Morgan, Craig John

2006-11-16T08:23:15Z
http://hdl.handle.net/10539/1768

Downloaded from a DSpace repository. https://dspace.org/

ANALYSING SPATIAL DATA VIA GEOSTATISTICAL METHODS

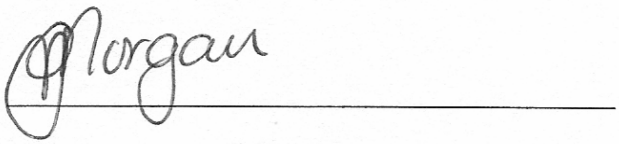
Craig John Morgan

A dissertation submitted to the Faculty of Science, University of the Witwatersrand, Johannesburg, in fulfillment of the requirements for the degree of Master of Science.

Johannesburg, 2005

DECLARATION

I declare that this dissertation is my own, unaided work. It is being submitted for the Degree of Master of Science at the University of the Witwatersrand, Johannesburg. It has not been submitted before for any degree or examination in any other University.



5th day of December 2005

ABSTRACT

This dissertation presents a detailed study of geostatistics. Included in this work are details of the development of geostatistics and its usefulness both in and outside of the mining industry, a comprehensive presentation of the theory of geostatistics, and a discussion of the application of this theory to practical situations. A published debate over the validity of geostatistics is also examined.

The ultimate goal of this dissertation is to provide a thorough investigation of geostatistics from both a theoretical and a practical perspective. The theory presented in this dissertation is thus tested on various spatial data sets, and from these tests it is concluded that geostatistics can be effectively used in practice provided that the practitioner fully understands the theory of geostatistics and the spatial data being analyzed. A particularly interesting conclusion to come out of this dissertation is the importance of using additive regionalized variables in all geostatistical analyses.

WitsETD

ACKNOWLEDGEMENTS

First of all, I wish to express thanks to my two supervisors, Professor Paul Fatti and Professor Dick Minnitt, for their assistance over the past three years. I would also like to thank Christina Dohm for supplying a sizeable spatial data set taken from the South African gold mining industry, and for allowing me to attend the three courses

1. Statistical Valuation of Ore Reserves (MINN 511)
2. Geostatistical Evaluation of Mineral Resources (MINN 510)
3. Practical Implementation of Geostatistical Evaluation (MINN 572)

given at the University of the Witwatersrand in 2003. Special thanks also goes out to Isobel Clark for making available the geostatistical computer package Geostokos Toolkit (c.2003), and for her general eagerness to help. Finally, I wish to thank the School of Statistics and Actuarial Science at the University of the Witwatersrand for financing the purchase of the geostatistical add-on package S+SpatialStats (2001).

WitsETD

CONTENTS

Page

DECLARATION ii

ABSTRACT iii

ACKNOWLEDGEMENTS iv

LIST OF FIGURES ix

LIST OF TABLES xix

LIST OF SYMBOLS AND COMMON NOTATION xxii

CHAPTER ONE – INTRODUCTORY CHAPTER 1

1.1 Introduction 1

1.2 An Elementary Description of Geostatistics 6

1.3 The History and Development of Geostatistics 7

1.4 Plan and Purpose for this Dissertation 9

1.5 Justification for this Study 10

1.6 A Preview of the Chapters to Follow 11

1.7 The Spatial Data used in this Dissertation 14

CHAPTER TWO – GEOSTATISTICS AND THE MINING INDUSTRY 15

2.1 Introduction 15

2.2 Mining Terminology 16

2.3 The Application of Geostatistics in the Mining Industry 19

2.4 Statistical Considerations when Applying Geostatistics in the Mining Industry 20

2.4.1 Support and the support effect 20

2.4.2 Statistical distributions 23

2.5 The Mining Industry in South Africa 24

CHAPTER THREE – CLASSICAL STATISTICAL THEORY IN GEOSTATISTICS 26

3.1 Introduction 26

3.2 The Distribution of the Sample Population 27

3.2.1 Construction of the sample histogram 27

WitsETD

3.2.2 The declustering technique 28
3.3 The Distribution of the Measured Attribute over other Supports 29
3.3.1 The affine correction model 29
3.4 The Lognormal Distribution 30
3.4.1 The two-parameter lognormal distribution 30
3.4.2 The three-parameter lognormal distribution 38
3.5 Grade-Tonnage Curves 42

CHAPTER FOUR – THE THEORY OF REGIONALIZED VARIABLES **51**
4.1 Introduction 51
4.2 The Probabilistic Model of Geostatistics 51
4.3 Assumptions 54
4.3.1 Second-order stationarity 54
4.3.2 Intrinsic stationarity 54
4.3.3 Ergodicity 55
4.4 Alternative Approaches to Spatial Estimation 57
4.4.1 Inverse distance weighting 57
4.4.2 Least squares regression 60
4.4.3 Polygonal estimation 61
4.4.4 Additional comments 63

CHAPTER FIVE – THE COVARIANCE FUNCTION AND THE VARIOGRAM **64**
5.1 Introduction 64
5.2 Valid Covariance Functions and Variograms 65
5.3 Additional Properties of Covariance Functions and Semi-variograms . 67
5.3.1 Mathematical properties 67
5.3.2 Continuity and differentiability 68
5.3.3 Behaviour near the origin 68
5.3.4 Behaviour further away from the origin 71
5.3.5 Isotropy and anisotropy 72
5.4 Commonly used Semi-variogram Models 76
5.4.1 The nugget effect model 77
5.4.2 The power model 77
5.4.3 The spherical model 78
5.4.4 The exponential model 79
5.4.5 The Gaussian model 79
5.4.6 Nested semi-variogram models 80

WitsETD

5.5 Estimation of the Semi-variogram 81
5.5.1 Method-of-moments estimator of the semi-variogram 81
5.5.2 The semi-variogram cloud 85
5.6 Fitting a Semi-variogram Model to the Estimated Semi-variogram . . . 86
5.7 Robust Estimates of the Semi-variogram 90
5.8 Relative Semi-variograms 91

CHAPTER SIX – EXPRESSIONS OF VARIANCE AND REGULARIZATION **93**
6.1 Introduction 93
6.2 Estimation Variance 94
6.2.1 Extension variance 94
6.2.2 Estimating a block by a weighted average 97
6.3 Dispersion Variance 99
6.3.1 Krige's relationship 101
6.4 Regularization 102
6.5 Calculation of $\bar{\gamma}(V,v)$ 105
6.5.1 Discretization 105
6.5.2 Auxiliary functions 107
6.6 The Effect of Nested Semi-variogram and Covariance Structures on the Estimation Variance, Dispersion Variance and Regularization . . . 113

CHAPTER SEVEN – KRIGING **115**
7.1 Introduction 115
7.1.1 The method of Lagrange multipliers for obtaining minima . . . 115
7.2 Ordinary Kriging 116
7.3 Simple Kriging 122
7.4 Kriging Weights 128
7.5 The Search Neighbourhood 136
7.6 Kriging as an Exact Interpolator 137
7.7 Kriging Variance 139
7.8 The Smoothing Effect 141
7.9 Cross Validation 142
7.10 Universal Kriging 143
7.11 Lognormal Kriging 149
7.12 Additional Issues in Kriging 153
7.12.1 Kriging using a relative (or proportional) semi-variogram model 153
7.12.2 Testing spatial data for the presence of trend 156

WitsETD

CHAPTER EIGHT – THE APPLICATION OF GEOSTATISTICAL THEORY **161**

8.1 Introduction 161
8.2 Decisions Regarding the Semi-variogram 164
8.2.1 Deciding on the type of semi-variogram model 166
8.2.2 The use of robust semi-variogram models 172
8.3 The Choice of Spatial Estimator 176
8.4 Additivity and the Logarithmic Transformation of Spatial Data – Theory and Application 182
8.4.1 Additivity and accumulation 183
8.4.2 The logarithmic transformation of lognormally distributed spatial data 186
8.4.3 Geostatistical analysis of the supplied gold mining data set . . . 188

CHAPTER NINE – THE PHILIP AND WATSON DEBATE **237**

9.1 Introduction 237
9.2 Summary of the Philip and Watson Debate 237
9.3 Critical Examination of the Philip and Watson Debate 247
9.4 Drawing Conclusions from the Philip and Watson Debate 252

CHAPTER TEN – CONCLUDING CHAPTER **255**

APPENDIX A – APPENDIX OF TABLES AND CHARTS **257**

APPENDIX B – ELEMENTARY STATISTICS **261**

B1 Basic Summary Statistics 261
B1.1 Measure of central tendency 261
B1.2 Measures of spread 262
B1.3 A measure of skewness 263
B1.4 A measure of ‘peakedness’ 264
B2 The Normal (Gaussian) Distribution 266

APPENDIX C – THE MATHEMATICS OF POSITIVE AND NEGATIVE DEFINITENESS **269**

REFERENCES **271**

WitsETD

LIST OF FIGURES

Page

Figure 1.1 The location of the nine random variables $Z(1)$, $Z(2)$, …, $Z(9)$ in two-dimensional Euclidean space. 1

Figure 1.2 The relationship between $\rho \in (0,1)$ and $9^{\#}$. The dotted line clearly shows that for $\rho = 0.2$ the nine correlated random variables provide the same precision in estimation of the overall mean μ as would be provided by 5.61 independent random variables. 5

Figure 2.1 An illustration of the difference between the statistical and geological concept of a sample, taken from Wellmer (1998 : 1). 18

Figure 2.2 A comparison of the distributions of values based on point and block supports, taken from Wackernagel (1995 : 55). Notice that the two distributions have the same overall average value, but due to averaging, the variability of the block distribution is smaller than that of the point distribution. 21

Figure 2.3 The proportion above cut-off for point and block support, taken from Wackernagel (1995 :56). Because the point support distribution has a larger variability and because cut-off is above the mean, a larger proportion of point support observations than block support observations will exist above the cut-off value. 21

Figure 3.1 The probability density function of $X \sim LN(2,\sigma^2)$ for $\sigma = 0.25$, 0.5, 0.75 and 1.00. This figure has been taken from Hogg & Tanis (1997 : 223) and shows the various shapes of the two-parameter lognormal distribution. It also illustrates that σ^2 is a good measure of spread of the lognormal distribution. 32

Figure 3.2 'Grade-tonnage' type curve displaying graphically the information contained in Table 3.1. 47

WitsETD

Figure 4.1 The location of the seven measured point support samples, as well as the location of the point to be estimated (which is indicated by the arrow). Figure 4.1 has been taken directly from Isaaks & Srivastava (1989 : 251). 58

Figure 5.1 Some common behaviours of semi-variograms near the origin. From left to right: parabolic behaviour; linear behaviour; discontinuity at the origin; pure nugget effect. Figure 5.1 is taken from Journel & Huijbregts (1978 : 39). . . 70

Figure 5.2 A typical semi-variogram function displaying a sill and a range. This figure has been taken from Armstrong (1998 : 26). 71

Figure 5.3 The example of geometric anisotropy and its elimination, as taken from Goovaerts (1997 : 91). 74

Figure 5.4 The example of zonal anisotropy and its elimination, as taken from Goovaerts (1997 : 94). 75

Figure 5.5 Basic shape of the nugget effect semi-variogram model. 77

Figure 5.6 The basic shape of the power semi-variogram models for a) $r = 1$ and b) $r < 1$ and $r > 1$. 78

Figure 5.7 The basic shape of the spherical semi-variogram model. 78

Figure 5.8 The basic shape of the exponential semi-variogram model. . . 79

Figure 5.9 The basic shape of the Gaussian semi-variogram model. 80

Figure 5.10 A flowchart by Armstrong (1998 : 49) demonstrating the procedure followed for obtaining a method-of-moments semi-variogram estimate. 83

Figure 5.11 Plots of the four directional method-of-moments semi-variogram estimates. These plots have been taken from Armstrong (1998 : 51). 85

WitsETD

Figure 5.12 The isotropic method-of-moments estimate of the semi-variogram. Armstrong (1998 : 52) mentions that "a linear [semi-variogram] model with a … nugget effect of about 3 gives a good fit [to this estimated semi-variogram]." 85

Figure 5.13 An example of a semi-variogram cloud taken from Wackernagel (1995). 86

Figure 5.14 a) A spherical semi-variogram model and b) a nested exponential semi-variogram model fitted to an experimental Cr concentration semi-variogram. Both models fit the experimental semi-variogram reasonably well. This figure is taken from Goovaerts (1997 : 100). 89

Figure 6.1 With $v \quad V$, this figure displays just some of the blocks of volume v that would be contained within the 'block' $V(x)$. . . 99

Figure 6.2 The point and regularized semi-variograms defined over a particular spatial region. Notice that for the larger modulus values of the vector h, the two semi-variograms simply differ in value by $\bar{\gamma}(v,v)$. This diagram has been taken from Journel & Huijbregts (1978 : 78). 104

Figure 6.3 The point support semi-variogram model for the metal accumulation in Example 6.1. This diagram is taken from Rendu (1981 : 30). 106

Figure 6.4 The 3×3 grid placed over the block $V(x)$ in Example 6.1. This diagram is also taken from Rendu (1981 : 30). 107

Figure 6.5 A line segment AB of length L. This figure is taken from Journel & Huijbregts (1978 : 108). 107

Figure 6.6 Rectangle ABCD with sides of length L and l. This figure is taken from Journel & Huijbregts (1978 : 109). 108

Figure 6.7 Visual summary of the four auxiliary functions defined in two dimensions. This figure has been taken from Rendu (1981 : 31), and the letters z' and z'' represent the two extremities of the vector h. 110

Figure 6.8 The location of the point support sample $z(x)$ and the block V. 111

WisETD

Figure 7.1 The data configuration of the five samples and the block to be estimated. 121

Figure 7.2 Situation 1: The location of the five point support samples $\{z(x_i)$: $i = 1$ to $5\}$ and the point to be estimated $z(x_0)$. 130

Figure 7.3 Situation 2: The location of the five point support samples $\{z(x_i)$: $i = 1$ to $5\}$ and the point to be estimated $z(x_0)$. 130

Figure 7.4 It is mentioned that the isotropic spherical covariance model in Equation 7.15 possesses a zero nugget effect and a unit sill. Now by introducing various nugget effect values, it can be seen how the ordinary kriging weights for the data configuration in Figure 7.3 are affected. The behaviour of the kriging weights discussed in the preceding paragraph is clearly displayed in this figure. Notice that when the entire unit sill is taken up by the nugget effect, all the kriging weights converge. The idea behind Figure 7.4 was taken from Goovaerts (1997 : 177). 133

Figure 7.5 The location of five point support samples $\{z(x_i)$: $i = 1$ to $5\}$ that will be used to estimate the point random variable $Z(x_0)$ via ordinary kriging. Note that in this illustration, the location x_0 is exactly the same as the location x_1 (i.e. the point to be estimated is located at the exact same point as one of the available samples). 138

Figure 7.6 The estimation of point A via kriging for two situations: one having consistent data values, the other having highly variable data values. Note that the data configuration of each of these situations is identical. 140

Figure 7.7 Example 7.3: Location of the five point support samples and the point to be estimated. 154

Figure 7.8 Plots associated with the example taken from Kaluzny et al. (1998). This figure is taken from Kaluzny et al. (1998 : 38). 157

Figure 7.9 A linear regression surface fitted to the available sample values. This figure is taken from Clark & Harper (2000 : 177). 158

Figure 7.10 Scatter-plot displaying the location and the relative value of the available samples. 159

WISER

Figure 7.11 The semi-variogram from Clark & Harper (2000 : 226) displaying a parabolic increase from a lag distance of about seventy meters. 159

Figure 8.1 Contour plot of the simulated regionalized variable possessing the underlying Gaussian semi-variogram. 166

Figure 8.2 Contour plot of the simulated regionalized variable possessing the underlying spherical semi-variogram. 166

Figure 8.3 The isotropic experimental semi-variogram of the simulated data set containing 144 point support samples. 167

Figure 8.4 The Fitted Gaussian semi-variogram model. 168

Figure 8.5 The fitted spherical semi-variogram model. 168

Figure 8.6 The ordinary kriging prediction surface assuming the Gaussian semi-variogram model in Figure 8.4. 169

Figure 8.7 The ordinary kriging prediction surface assuming the spherical semi-variogram model in Figure 8.5. 169

Figure 8.8 A spherical semi-variogram model with a nugget effect fitted to the experimental semi-variogram displayed in Figure 8.3. 171

Figure 8.9 The ordinary kriging prediction surface assuming the nugget inclusive spherical semi-variogram model in Figure 8.8. 171

Figure 8.10 Histogram of the 144 point support values of the simulated spatial data set introduced in Section 8.2.1. 172

Figure 8.11 Histogram of the 144 point support values of the simulated spatial data set introduced in Section 8.2.1 after two of the values were replaced by larger outlying values. These two outliers can clearly be seen in this histogram. 173

Figure 8.12 The experimental semi-variogram of the simulated data set with two of the 144 values replaced by larger outliers. 174

WitsETD

Figure 8.13 The robust experimental semi-variogram of the outlier inclusive simulated data set, together with a fitted spherical semi-variogram model (cf. Figure 8.5). 176

Figure 8.14 Histogram of the 94 true values. 178

Figure 8.15 Histogram of the 94 polygonal estimates. 178

Figure 8.16 Histogram of the 94 inverse distance weighting estimates. . . 178

Figure 8.17 Histogram of the 94 ordinary kriging estimates. 178

Figure 8.18 Histogram of the estimation errors associated with the polygonal estimates. 180

Figure 8.19 Histogram of the estimation errors associated with the inverse distance weighting estimates. 180

Figure 8.20 Histogram of the estimation errors associated with the ordinary kriging estimates. 180

Figure 8.21 The spatial location of all 2321 point support gold-ore samples. 183

Figure 8.22 The spatial location of the 2321 point support samples of the gold mining data set provided by Dr. Dohm. The 384 red-coloured points represent the samples that will be removed from this data set. These samples are located in six distinct zones (or blocks, see Note 8.12). The remaining 1937 black-coloured samples will be used to re-estimate the gold grade at the location of each of the removed (red-coloured) samples. . 190

Figure 8.23 Histogram of the gold-ore grade of the 1937 point support samples. 191

Figure 8.24 Histogram of gold-ore thickness of the 1937 point support samples. 191

Figure 8.25 Histogram of the gold-ore accumulation of the 1937 point support samples. 191

WitsETD

Figure 8.26 A histogram of the available 1937 ln[$y(x)$] values. The histogram displays a skewness of 0.04 and a kurtosis of 2.73. 199

Figure 8.27 The isotropic nested spherical semi-variogram model fitted to the experimental semi-variogram calculated from the 1937 ln[$y(x)$] values. This semi-variogram model is a combination of two spherical semi-variogram models, and also displays a relatively large nugget effect. Note that the size of the symbols ⊕ is proportional to the number of sample pairs used to obtain that point. 200

Figure 8.28 A histogram of the available 1937 ln[$u(x)$] values. The histogram displays a skewness of 0.04 and a kurtosis of 2.57. 202

Figure 8.29 The isotropic nested exponential semi-variogram model fitted to the experimental semi-variogram calculated from the 1937 ln[$u(x)$] values. This semi-variogram model is a combination of two exponential semi-variogram models, and also displays a relatively large nugget effect. Note again that the size of the symbols ⊕ is proportional to the number of sample pairs used to obtain that point. 202

Figure 8.30 The cubic trend surface over the ore deposit, fitted to the 1937 gold-ore thickness values by Geostokos Toolkit (c.2003). 203

Figure 8.31 The isotropic spherical semi-variogram model fitted to the experimental semi-variogram calculated from the 1937 cubic surface residuals of the gold-ore thickness. 204

Figure 8.32 The isotropic experimental semi-variogram calculated from the 1937 untransformed gold-ore grade sample values. 205

Figure 8.33 The spatial study area (i.e. the gold-ore deposit), which contains 1937 point support sample values (represented by the grey dots), is divided into nine non-overlapping rectangular zones in order to test for the presence of a proportional effect. All nine zones are of equal size and measure 150 Eastings x 175 Northings. 206

Figure 8.34 Scatterplot of the local mean versus the local standard deviation for each of the nine zonal areas in Figure 8.33 (see Table 8.5). The correlation between the local mean and the local standard deviation is calculated as 0.89. 207

WiSER

Figure 8.35 The nine experimental gold-ore grade semi-variograms for each of the nine non-overlapping zones (see Figure 8.33) and the local relative gold-ore grade experimental semi-variogram calculated from these nine experimental semi-variograms. . . 208 to 210

Figure 8.36 The nested exponential semi-variogram model fitted to the local relative experimental semi-variogram. 210

Figure 8.37 Scatterplot of the local gold-ore accumulation mean versus the local gold-ore accumulation standard deviation for each of the nine zonal areas in Figure 8.33. The correlation between the local mean and the local standard deviation is calculated as 0.76. 212

Figure 8.38 The nine experimental gold-ore accumulation semi-variograms for each of the nine non-overlapping zones in Figure 8.33, and the local relative gold-ore accumulation experimental semi-variogram calculated from these nine experimental semi-variograms. . . . . 214 and 215

Figure 3.39 The nested exponential semi-variogram model fitted to the local relative experimental semi-variogram in Figure 8.38. . . 216

Figure 8.40 The isotropic nested exponential semi-variogram model fitted to the experimental semi-variogram calculated from the 1937 available gold-ore grade values. This semi-variogram model is a combination of two exponential semi-variogram models, and also displays a nugget effect. 217

Figure 8.41 The isotropic nested exponential semi-variogram model fitted to the experimental semi-variogram calculated from the 1937 gold-ore accumulation values. This semi-variogram model is a combination of two exponential semi-variogram models, and also displays a nugget effect. 219

Figure 8.42 A histogram showing the true gold-ore grade distribution of the 384 point support samples that are to be re-estimated by each of the six geostatistical analyses. 220

Figure 8.43 a) A histogram of the 384 point support gold-ore grade estimates produced by Geostatistical Analysis 1, and b) A histogram of the 384 estimation errors (i.e. the true gold-ore grade less the estimated gold-ore grade), associated with Geostatistical Analysis 1. 221

VIEW

Figure 8.44 a) A histogram of the 384 point support gold-ore grade estimates produced by Geostatistical Analysis 2, and b) A histogram of the 384 estimation errors (i.e. the true gold-ore grade less the estimated gold-ore grade), associated with Geostatistical Analysis 2. 221

Figure 8.45 a) A histogram of the 384 point support gold-ore grade estimates produced by Geostatistical Analysis 3, and b) A histogram of the 384 estimation errors (i.e. the true gold-ore grade less the estimated gold-ore grade), associated with Geostatistical Analysis 3. 221

Figure 8.46 a) A histogram of the 384 point support gold-ore grade estimates produced by Geostatistical Analysis 4, and b) A histogram of the 384 estimation errors (i.e. the true gold-ore grade less the estimated gold-ore grade), associated with Geostatistical Analysis 4. 222

Figure 8.47 a) A histogram of the 384 point support gold-ore grade estimates produced by Geostatistical Analysis 5, and b) A histogram of the 384 estimation errors (i.e. the true gold-ore grade less the estimated gold-ore grade), associated with Geostatistical Analysis 5. 222

Figure 8.48 a) A histogram of the 384 point support gold-ore grade estimates produced by Geostatistical Analysis 6, and b) A histogram of the 384 estimation errors (i.e. the true gold-ore grade less the estimated gold-ore grade), associated with Geostatistical Analysis 6. 222

Figure 8.49 Scatterplots of the logarithms of the 384 estimated gold-ore grades versus the logarithms of the associated 384 true gold-ore grades, for each of the six geostatistical analyses. 227

Figure 8.50 Scatterplot of the logarithms of the 384 estimated gold-ore grades versus their associated 384 estimation errors for Geostatistical Analysis 2. The larger estimates are often associated with large positive errors. This is a direct consequence of the smoothing effect on the kriging estimates and the skew distribution of the true gold-ore grade values in Figure 8.42. 228

WitsETD

Figure A1 A chart for the auxiliary function $H(L\ ;\ l)$ of a spherical semi-variogram model with a sill and range value equal to one. The letter a in the axes refers to the range parameter of the non-standardized spherical semi-variogram model (see Equation 5.14). This chart is taken from Journel & Huijbregts (1978 : 127). 260

Figure B1 An example of a positively skew, symmetric and negatively skew distribution. 264

Figure B2 An example of a leptokurtic and a platykurtic distribution. . . 265

Figure B3 A normal probability distribution with mean μ and standard deviation σ^2, taken from Clark & Harper (2000 : 32). 266

WitsETD

LIST OF TABLES

		Page
Table 2.1	South Africa's mineral reserves, 2001 (from Burger, c.2003).	25
Table 3.1	Table showing the proportion of the polluted area above the pollution cut-off level as well as the average pollution value of these regions, for a number of possible pollution cut-off values.	47
Table 4.1	Inverse distance weighting calculations for estimating the point $z(x_0)$, using the seven available sample values in Figure 4.1.	59
Table 4.2	The regression equation fitted to describe the proportion of pyritic sulphur in a certain type of coal (taken from Armstrong, 1998 : 17).	61
Table 5.1	The location of all sixty four values. This table is taken from Armstrong (1998 : 51).	84
Table 5.2	Calculations of $\hat{\gamma}(h)$ for various distances and directions, for the data in Table 5.1. The values in this table were taken directly from Armstrong (1998 : 51). Note that the values $N(h)$ correspond to the number of sample pairs associated with each of the lag distances h (see Equation 5. 19).	84
Table 5.3	Calculation of the isotropic semi-variogram values $\hat{\gamma}(h)$ for various distances, for the data in Table 5.1.	85
Table 8.1	Summary of the distribution of the 94 true values, the 94 polygonal estimates, the 94 inverse distance weighting estimates, and the 94 ordinary kriging estimates.	178
Table 8.2	Summary of the estimation error distribution associated with the polygonal estimation, inverse distance weighting estimation and ordinary kriging estimation.	180
Table 8.3	Summary statistics of gold-ore grade, gold-ore thickness and gold-ore accumulation of the 1937 point support samples.	192

WitsETD

Table 8.4 Summary of the assumptions of the six geostatistical analyses. 197

Table 8.5 A table giving the local mean and the local standard deviation of gold-ore grade values within each zone, as well as the number of samples contained within each zone. 206

Table 8.6 Table giving the local mean and the local standard deviation of the gold-ore accumulation sample values within each zone, as well as the number of samples contained within each zone. 212

Table 8.7 Various summary statistics calculated for each of the six geostatistical analyses. 224

Table 8.8 Ranking of the performance of the six geostatistical analyses for each of the seven summary statistics presented in Table 8.7. A ranking of one is associated with the geostatistical analysis that performed the best with respect to the measured statistic; a ranking of six is associated with the geostatistical analysis that performed worst. The final row in this table gives the sum of the rankings for each of the geostatistical analyses. 229

Table 8.9 A summary of the relative performance of the six geostatistical analyses with respect to the sum of the rankings (see Table 8.8), the median squared error, and the median absolute error (see Table 8.7). 231

Table 8.10 Summary of the conclusions drawn from the comparison of the six geostatistical analyses in Section 8.4.3. 234

Table 8.11 Mean and median average percentage error calculated for each of the six geostatistical analyses studied in Section 8.4.3. 236

Table A1 Table of $\gamma_n(V_y)$ for various values V_y and n, taken from Sichel (1966 : 117-118). 257

Table A2 Table of $\psi_{0.05}(V_y\ ,\ n)$ and $\psi_{0.95}(V_y\ ,\ n)$, taken from Sichel (1966 : 119). 258

Table A3 Cumulative distribution of the standard normal distribution taken from Hogg & Tanis (1997). 259

WiSER

Table A4 Various values of the auxiliary function $H(L;B)$ for a spherical model with sill and range value equal to one. This table is taken from Clark (1979 : 82). 260

WitsETD

LIST OF SYMBOLS AND COMMON NOTATION

	indicate the conclusion of a proof
	indicates the conclusion of an example
	indicates the conclusion of a note
$\alpha(L\,;\,l)$	an auxiliary function
β	the threshold parameter of a three-parameter lognormal distribution
β_1	the square of the population skewness
β_2	the population kurtosis
c_0	a nugget-effect
$C(0)$	the covariance value at a lag of zero; equal to the variance of a second-order stationary random function
$C(h)$	a covariance function
$\chi(L)$ and $\chi(L\,;\,l)$	auxiliary functions
$C_V(h)$	the regularized covariance function of support V, i.e. the covariance function of a random function of support V
$\overline{C}(V,v)$	the mean value of $C(h)$ when one extremity of vector h describes the domain $V(x)$ and the other extremity independently describes the domain $v(y)$
$C(x,y)$ or $\mathrm{cov}(x,y)$	the covariance between the random variables $Z(x)$ and $Z(y)$

WitSETD

$D^2(v/V)$	the dispersion variance of blocks $v(y)$ within $V(x)$
$\mathrm{E}\{Z(x)\}$	the expectation of a random function or a random variable
$F(L)$ and $F(L\,;\,l)$	auxiliary functions
$f(x)$	generally indicates a function of the spatial co-ordinate x, or a probability density function
$\gamma(h)$	a semi-variogram. $2\gamma(h)$ is the notation for a variogram.
$\gamma_V(h)$	the regularized semi-variogram of support V, i.e. the semi-variogram of a random function of support V
$\gamma(x,y)$	the semi-variogram value between the random variables $Z(x)$ and $Z(y)$
$\bar{\gamma}(V,v)$	the mean value of $\gamma(h)$ when one extremity of the vector h describes the domain $V(x)$ and the other extremity independently describes the domain $v(y)$
h	a separation vector of modulus $\|\|h\|\|$
$H(L\,;\,l)$	an auxiliary function
$\lambda_i\,,\,\lambda_j\,,\,\ldots$	generally refers to kriging weights or the weights of a linear combination
μ	the population mean
$N(h)$	indicates the set containing all sample pairs separated by the vector h
OK	ordinary kriging
OLK	ordinary lognormal kriging
Ω	a spatial study area of two- or three-dimensions

WitsETD

$\Phi(y)$	the cumulative distribution function of the standard normal distribution
^{1}, ^{2}, ^{3}	one-, two- and three dimension Euclidean space respectively
σ^2	the population variance
σ_E^2	the estimation variance
$\sigma_E^2(v,V)$	the extension variance of v to V
σ_{OK}^2	the ordinary kriging variance
σ_{OLK}^2	the ordinary lognormal kriging variance
σ_{SK}^2	the simple kriging variance
σ_{UK}^2	the universal kriging variance
SK	Simple kriging
t	Sichel's t-estimator
τ	the mean value of a two- or three-parameter lognormal distribution
UK	universal kriging
var$\{Z(x)\}$	the variability of a random function or a random variable
$V(x)$	A volume (or area) V centred at the point location x
$v(x)$	a volume (or area) v, usually smaller than V, centred at the point location x
ϖ, ϖ_i	Lagrange multipliers
$x, y, \ldots$	generally indicates a point co-ordinate in one-, two- or three-dimensional space

WitsETD

$Z_V(x)$	a block support random function or random variable, with a support volume (or area) of V
$z_V(x)$	a block support regionalized variable or a realization of a block support random variable, with a support volume (or area) of V
$Z(x)$, $Y(x)$, …	a random function or a random variable at the point location x
$z(x)$, $y(x)$, …	a regionalized variable or a realization of a random variable at the point location x

WitsETD